

Gravitational microlensing of fractal sources

Geraint F. Lewis

Institute of Astronomy, School of Physics, University of Sydney, NSW 2006, Australia: gfl@physics.usyd.edu.au

12 October 2018

ABSTRACT

Gravitational microlensing has proven to be a powerful tool in the study of quasars, providing some of the strongest limits on the scales of structure in the central engine. Typically sources are considered to be smoothly varying on some particular scale; such simple sources result in recognisable time scales in microlensing light curves from which the size of the source can be determined. Various emission processes, however, result in sources with a fractal appearance, possessing structure on a range of scales. Here, the gravitational microlensing of such fractal sources at the heart of quasars is considered. It is shown that the resulting light curves reflect the fractal nature of the sources, possessing pronounced structure at various scales, markedly different to the case with the random distribution of emission clouds that are typically considered. Hence, the determination of a characteristic scale of variability in a microlensing light curve may not necessarily reveal the size of the individual emission clouds, the key value that is required to determine the physical state of the emission region, rather it may correspond to a particular hierarchy in a fractal structure. Current X-ray satellites can detect such fractal structure via the monitoring of gravitationally lensed quasars during a microlensing event, providing a test of high energy emission processes in quasars.

Key words: gravitational lensing – quasars: emission lines – quasars: absorption lines

1 INTRODUCTION

Quasars represent some of the most luminous objects in the universe. While their spectra reveal clues to the various emission regions within the active nucleus, their small angular size at cosmological distances means that we are not able to directly image their central regions. New clues have come from quasars which have been magnified by gravitational microlensing, and observations of microlensing events have provided strong constraints on the relative sizes of the quasar emission regions (Rauch & Blandford 1991; Lewis, Irwin, Hewett & Foltz 1998; Agol, Jones & Blaes 2000; Yonehara 2001). Recent studies have focused upon the influence of obscuring material in the broad absorption line region (Lewis & Belle 1998) and in the extensive broad emission line region (Wyithe & Loeb 2002) as the continuum source is microlensed. These studies have found that the shadowing of the emission/absorption clouds produces pronounced signatures on the microlensing light curve, and the scale of these signatures can be used to infer the size of the obscuring clouds.

Typically in microlensing studies, emission and absorption regions are deemed to have a simple brightness profile and scale, and problems focus upon determining these scales from observations of fluctuations induced by gravitational

microlensing. In recent years, however, it has been realised that many natural processes are fractal in nature, possessing similar structural properties on a variety of scales. This paper presents an investigation of the influence of fractal structure on the properties of microlensing light curves, especially with regard to the determination of the scale of structure of a particular emission region. In Section 2, fractals in astronomy are briefly reviewed, outlining the physical motivation of the model adopted in this paper, while in Section 3.1 the approach adopted to study the gravitational microlensing of fractal clouds is presented, whereas the results are presented in Section 4. The conclusions are discussed in Section 5.

2 ASTRONOMICAL FRACTALS & FRACTAL SOURCES

The fact that a large number of natural phenomenon appear to possess fractal structure, displaying self-similarity on a range of scales, has been known for sometime (e.g. Peitgen & Richer 1986; Peitgen & Saupe 1988). Such structure has been observed in various astrophysical contexts, from the surface of Mars (Stepinski et al. 2002), the distribution of asteroids (Campo Bagatin et al. 2002), and the influence of fractal dust grains (Wright 1989; Fogel & Leung 1998). One

arXiv:astro-ph/0408196v1 11 Aug 2004

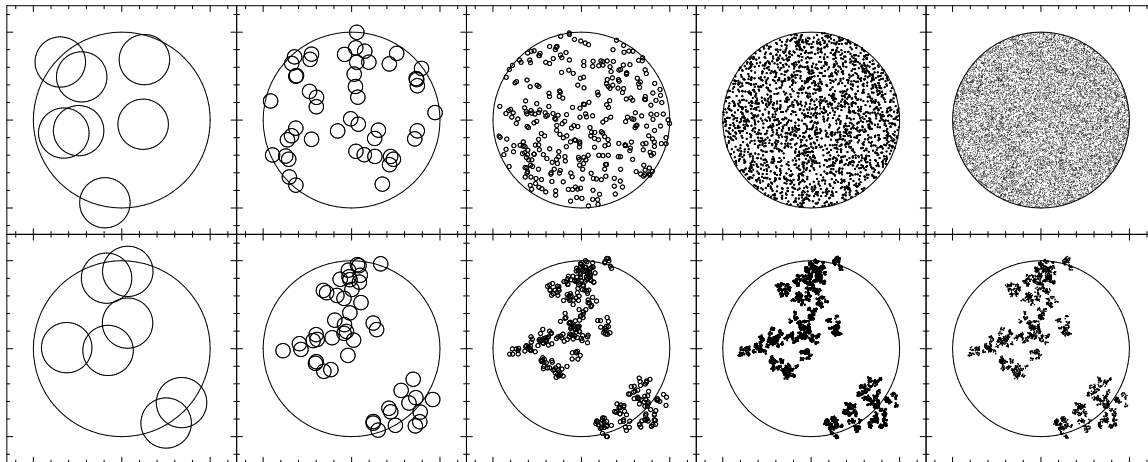


Figure 1. The lower row of panels presents a series of fractal hierarchies for the source structure discussed in this paper, beginning with level 1 on the left-hand side to level 5 on the right-hand side. The upper series of panels presents random distributions of the same number and size of clouds seen in the lower panels. At the lowest hierarchical levels (left-hand panels) the distributions are similar in the random and fractal cases, but as higher hierarchical levels are considered, the clumping in the fractal distribution ensures it rapidly deviates from the random distribution of clouds. The large circle in each panel corresponds to the lowest (zeroth) fractal hierarchy, of radius R_{max} .

of the longest running debates has involved the question of whether large scale structure in the universe is fractal in nature¹, as such a conclusion would invalidate the central ideas of relativistic cosmology (e.g. Durrer & Labini 1998).

Many astrophysical studies of fractal distributions have been concerned with self-similar structure in gas clouds (e.g. Elmegreen 1997; Stutzki et al. 1998; Elmegreen et al. 2001; Elmegreen 2002; Datta 2003) or in stellar distributions (Elmegreen & Elmegreen 2001). While these studies may seem somewhat esoteric, with fractal analyses providing useful classification tools (e.g. Lekshmi et al. 2003), the existence of fractal structure influences the evolution of both gaseous (Semelin & Combes 2002) and stellar (Goodwin & Whitworth 2004) components. Furthermore, Bottorff & Ferland (2001) examined the broad-line region of quasars, suggesting that transient, turbulence-induced overdensities within the emission region would possess fractal structure, complicating the interpretation of the physical properties of the region.

Fractal processes have also been associated with Sun, including its global activity (Salakhutdinova 1998), radio bursts (Veronig, Messerotti & Hanslmeier 2000) and large-scale magnetic field (Burlaga, Wang & Ness 2003). The small-scale magnetic structure too appears to possess many fractal features (Abramenko 1999; Stenflo & Holzreuter 2003; Janßen, Vögler & Kneer 2003). In quasars, the X-ray emission arises from the most central regions, amidst a complex and dynamic magnetic field structure in an accretion disk corona (e.g. Merloni & Fabian 2001a), similar to the activity seen in the Solar corona. Cascades of activity in such regions may result in fractal like emission (Merloni & Fabian 2001b). Given that the small X-ray emitting region at the centres of quasars are amenable to microlensing (Yonehara et al. 1998), this paper explores microlensing signatures of a

quasar X-ray emission region with a fractal surface brightness distribution.

3 METHOD

3.1 Gravitational Microlensing

The fluctuations in brightness induced by a gravitational lensing mass depend implicitly on its caustic structure. An isolated, point-like mass, such as a MaCHO within the Galactic halo, produces a point-like caustic. This results in a simple, smoothly varying light curve (e.g. Alcock et al. 1993). Multiple stars, however, can combine in a very non-linear fashion, leading to an extended caustic structures and more complex light curves (e.g. Alcock et al. 2000). At optical depths around unity, where many individual lenses combine to influence the light from a distant source, the resulting caustic structure, and hence brightness fluctuations, are quite complex (see Kayser, Refsdal & Stabell 1986; Wambsganss 1992); this situation is applicable to microlensed quasars such as Q2237+0305 (Wambsganss, Paczynski & Katz 1990). An examination of such complex caustic structures reveals that they are dominated by fold catastrophes which link the higher order catastrophes (Witt 1990). For the purposes of this paper, it is assumed that the source under consideration is small compared to the overall caustic structure, such that the source can be seen to be swept by single a fold caustic, an assumption which hold for the X-ray emitting regions of quasars (Yonehara et al. 1998). It is also assumed that the caustic is straight on the scale of the overall source structure, such that higher order curvature effects (Fluke & Webster 1999) can be neglected. With this, the magnification of a fold caustic is simply given as;

$$\mu(x) = \sqrt{\frac{g}{x - x_c}} H(x - x_c) + \mu_o \quad (1)$$

¹ See <http://pil.phys.uniroma1.it/astro.html> for a description of the debate.

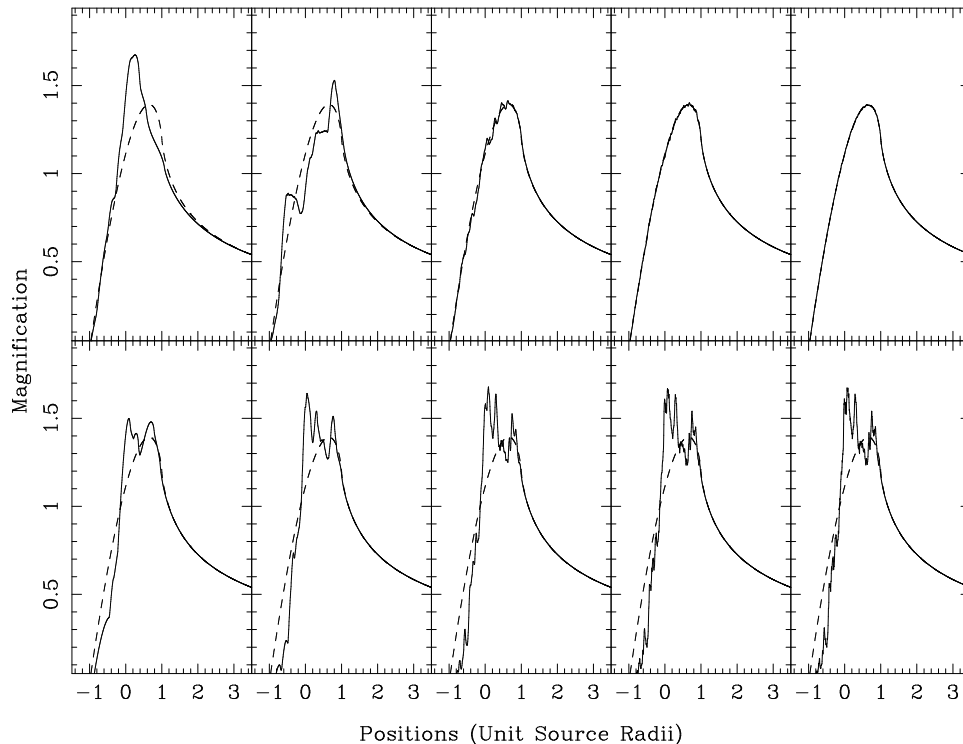


Figure 2. The result of sweeping the caustic from left to right over the cloud distributions presented in Figure 1. In each panel, the dashed line corresponds to the light curve for a uniform source of unit radius. In the upper panels, which present the combined light curves of randomly distributed sources, the total light curve rapidly matches that of the single uniform source. The lower panels present the light curves for the fractally distributed sources. Clearly, the behaviour of this light curve is different to the random case.

where $x - x_c$ represents the perpendicular distance to the caustic, $H(x)$ is the Heaviside step function and g is the “strength” of the caustic (Witt 1990). The μ_o term accounts for the flux from the other images caused by the caustic network and is assumed to be constant in the vicinity of the caustic; this is taken to be zero for this study without any loss of generality. The clouds² are considered to be circular and of uniform surface brightness. In calculating the resulting brightness fluctuation as a source is swept by a fold caustic, the analytic expressions of Schneider & Wagoner (1987) are employed, setting their limb darkening parameter, $c_+ = 0$.

Chang (1984) demonstrated that a source of radius R which is swept by a fold caustic suffers a maximum magnification of;

$$\mu_{max} = \sqrt{\frac{g}{R}} f \quad (2)$$

where f is a form factor, which accounts for the specific shape and surface brightness distribution of a source. For the uniform, circular sources under consideration in this paper, $f = 1.39$. The caustic strength g is assumed to be unity throughout this analysis. Detail of the physical scaling of this model to observed microlensing situations can be found in Lewis & Belle (1998).

² For this paper, clouds refers to regions of emission. While the studies of Lewis & Belle (1998) and Wyithe & Loeb (2002) considered absorbing clouds in front of a continuum source, the results presented in this paper can be scaled to this case.

3.2 Cloud Distributions

In producing a fractal cloud distribution, several parameters are required; the geometric factor (L) relates the scale of substructure within a structure, such that a structure of size R will possess substructures of size RL^{-1} . The multiplicity, N , is the number of such substructures within a structure; these parameters define the fractal dimension of the distribution with $D = \log N / \log L$. The maximum hierarchy, H , is the number of scales of substructure considered. With this, the radius of the smallest substructures (equivalent to individual clouds) is;

$$R_{cloud} = R_{max} L^{-H} \quad (3)$$

where R_{max} is the radius of the largest scale of the hierarchy, corresponding to the radius of the overall region being microlensed. Similarly, the scale of each hierarchy is;

$$R(h) = R_{max} L^{-h}, \quad h = 0, 1 \dots H \quad (4)$$

where $h = H$ corresponds to the individual clouds, and $h = 0$ is the lowest level of the fractal hierarchy, corresponding to a radius of R_{max} .

Hence, in generating the fractal distribution, N subregions of size $R = R_{max} L^{-1}$ are randomly scattered into the zeroth level hierarchy, within a radius of R_{max} . Within these subregions, N further subregions of size $R = R_{max} L^{-2}$ are scattered. The procedure is continued until the subregions represent the individual clouds themselves [see Bottorff & Ferland (2001) for a further description of this procedure].

To date, there are no detailed models to predict precise fractal X-ray surface brightness distributions within the

central regions of quasars. To this end, the fractal distributions presented here are illustrative only, not driven by any particular physical constraints. A fractal model was chosen with $L = 3.5$ and a fractal dimension of $D = 1.55$, corresponding to 7 structures per level. The lower panels of Figure 1 presents the spatial distributions of the could distributed with these fractal parameters; from the left to right, the panels present the first to the fifth hierarchy of fractal structure; the large circle in all panels corresponds to the lowest (zeroth) level of the fractal hierarchy and has a radius of R_{max} . The lower left-most panel presents the case with $h = 1$, the first fractal hierarchy. Here there are seven source regions randomly scattered within R_{max} , each with a radius of $R_{cloud} = R_{max}L^{-1} \sim 0.29R_{max}$. In the panel immediately to the right, the second fractal hierarchy, $h = 2$, is considered, and each of the emission clouds in the $h = 1$ level has been broken up into seven smaller clouds, each with a radius of $R_{cloud} = R_{max}L^{-2} \sim 0.08R_{max}$, with each cloud being randomly scattered within the circle of the $h = 1$ cloud. This process to $h = 5$ in the right-most panel. This right-most panel consists of $7^5 = 16807$ individual emission clouds, each with a radius of $R_{cloud} = R_{max}L^{-5} \sim 0.002R_{max}$. The upper panels consider a similar procedure, but instead of scattering clouds in each hierarchy within the boundaries defined by the hierarchy below it, the clouds are scattered randomly within R_{max} , providing an overall random distribution. It is immediately apparent that the fractal distributions differ significantly from the random distributions and possess structure on a number of scales (as expected for fractal distributions).

4 RESULTS

4.1 Microlensing Light Curves

Figure 2 presents the microlensing light curves for the sources at each hierarchy presented in Figure 1; note that for the simulations presented in this paper, it is assumed that the source region remains fixed and unvarying as it is swept by the microlensing caustic; such variability would further complicate the resulting light curve, confusing the microlensing signature. The dashed line in each panel corresponds microlensing light curve for a source of unit radius, corresponding to R_{max} in this case, and the surface brightness of each source hierarchy has been adjusted so that it matches this light curve after the caustic has passed the emission region. In the left-most panel, the source region consists of a small number of relatively large sources, a situation which is reflected in the light curve, which exhibits substantial variations about the unit radius source light curve. Moving towards the right of the top panels of Figure 2, as the source size decreases and their number increases, the size of the deviations from the unit source decreases, becoming imperceptible in the final frame of the panel, representing the resultant light curve of 16807 randomly distributed sources.

Considering the lower panels of Figure 2 reveals that, as expected, the lowest fractal hierarchy produces a similar light curve to the random distribution of sources, a situation which is apparent in the second hierarchy. In moving to higher fractal hierarchies (towards the right), however, it is seen that there is a pronounced difference between the

light curves from the fractal distributions and the random distributions, with the light curves of the fractal sources not approaching that of the unit circular source. Rather, as higher hierarchies are considered, it is seen that structures that appear in lower hierarchies persists.

This behaviour is straight forward to understand; for the random distributions, additional sources added at each hierarchy act to *fill the gaps* in the light curve, eventually smoothing the light curve out to the uniform source (as seen in the right-most panel of Figure 2). For the fractal source, however, the smaller sources in the higher hierarchies are constrained to lie in the regions of the lower hierarchies. This ensures that each higher fractal level effectively maintains the larger scale variability of the preceding hierarchy, adding smaller scale variability to it.

Note that in this example the fractal hierarchy has only been considered down to fifth level. In reality, the fractal hierarchy can be substantially deeper [c.f. Bottorff & Ferland (2001) who find that the broad line region of quasars is best represented by a fractal with eleven hierarchies, corresponding to a total $\sim 10^{10}$ individual emission clouds]. If this is the case, then the light curve presented for the random distributions would appear quite smooth and would do so until explored on the scale of the very high hierarchies. The fractal distribution would, however, continue to display variability on all the scales of the fractal distribution.

4.2 Implications

A number of studies have attempted to determine the scale size of continuum emitting region in quasars using the time scale of gravitational microlensing variability (Wyithe, Webster & Turner 2000; Yonehara et al. 1999; Kochanek 2004), including specifically the X-ray emitting region (Yonehara et al. 1998; Popović et al. 2003). All these studies, however, assume a simple source profile.

Would a fractal source result in any observational consequences? To examine this it is important to consider the time scale of microlensing variability. For the quadruple lens Q2237+0305, the caustic crossing time scale is

$$t \sim \left(\frac{r_{src}}{4 \times 10^{13} \text{cm}} \right) \left(\frac{v_t}{600 \text{km/s}} \right)^{-1} \text{ days} \quad (5)$$

where r_{src} is the radius of the source and v_t is the transverse velocity of the lensing galaxy (Kayser et al. 1998; Yonehara et al. 1998). Confined to the inner regions of the accretion disk, the X-ray emitting region is estimated to be $\sim 10 - 20$ Schwarzschild radii in extent (e.g. Merloni & Fabian 2001), corresponding to $\sim 3 \times 10^{14}$ cm for a $10^8 M_\odot$ black hole. Clearly, given Equation 5, the light curves presented in Figure 2 are ~ 1 month in duration. It is important to note, however, that all the light curves are smooth beyond unity along the spatial axis, corresponding to times when the sharp boundary of the fold caustic has swept completely across the entire source region. Hence, strong variability due to the fractal structure of the source can only be seen when this high magnification region lies across the source, confining the strong variability to a period of a couple of weeks. To obtain a signal-to-noise of ~ 10 in the faintest images of Q2237+0305, Chandra need to integrate for ~ 15 ks (Dai et al. 2003), implying a temporal resolution of $\sim 4 - 5$ hours

and, via Equation 5, a spatial resolution of $\sim 7 \times 10^{12}$ cm; this corresponds to the third hierarchical level ($h = 3$) for the fractal distribution considered in this paper. Hence, with this temporal sampling and 10% photometry, the fractal nature of the source would be imprinted on the observed light curve.

Given the self-similar structure in the source, and hence in the light curve, any observing period shorter than the total caustic crossing displayed in Figure 2 may identify variability that is interpreted as revealing the scale size of the X-ray emission region, whereas it truly corresponds to a particular level in the fractal hierarchy; this will be especially true if the data are noisy, masking any variations introduced due to the substructures in higher fractal hierarchies. In searching for the full fractal signature, therefore, it is imperative to following the entire sweeping of the source region during a microlensing event. As the optical/UV emission region should be substantially larger than the X-ray emitting region, any microlensing in the optical/UV should possess a proportionally larger time scale. Hence, monitoring at these longer wavelengths could be used to identify microlensing events, and providing a trigger for monitoring in the X-ray.

Of course, it is important to note that the fractal distribution discussed in this paper does not represent a specific model for the X-ray surface brightness in quasars. While the particular imprint of a fractal source on a microlensing light curve depends upon the details of the distribution, it is expected that any resulting light curve will possess self-similar structure on a range of scales. This can be used to determine the physical validity of models for quasar X-ray emission (e.g. Merloni & Fabian 2001b).

5 CONCLUSIONS

Studies of the gravitational microlensing of quasars typically assume that source are smooth, possessing a typical scale-length that can be determined from observations of microlensing variability. Over the last decade, it has become clear that a number of physical processes can result in structures with fractal properties. This has included high energy emission from the solar corona and, in an analogous model, to X-ray emission from the heart of quasars.

This paper has considered the influence of fractal structure in the X-ray emitting region of quasars as it is swept by a caustic during a microlensing event. It was found that, for a random distribution of clouds, as the size of the clouds were decreased, and their number increased, the total light curve rapidly approached that of a larger uniform source. Sources distributed fractally, however, displayed quite different properties; as the source size is decreased and the number of clouds increased, they are not distributed randomly, but within fractal hierarchies. This clustering of sources is quite apparent in the resultant light curve, with higher fractal hierarchies adding variability substructure to the lower hierarchies. Unlike the randomly distributed sources, the light curve does not resemble that of a larger, uniform source, but (like the source itself) possesses substructure on a range of scales. An examination of the relevant time scales reveals that monitoring of gravitationally microlensed quasars with X-ray satellites would allow the determination of the lower

levels of fractal structure, providing further tests to the underlying emission mechanisms.

The small, X-ray emitting regions of quasars are not the only structures in active galaxies that possess fractal structure, with Bottorff and Ferland (2001) suggesting that the extensive broad line emitting region should also be fractal in nature. Microlensing of the broad line region was examined by Nemiroff (1988) and Schneider & Wambsganss (1990) who found that due to the overall size of the emission region (\sim parsec scale) the flux in the emission line is essentially unaltered due to the action of gravitational microlensing, although microlensing could result in variability of the emission line profiles. Reverberation mapping experiments have suggested an overall smaller size for the broad line region (~ 0.1 parsecs), further indicating that the region should be amenable to strong gravitational microlensing (Abajas et al. 2004; Lewis & Ibata 2004). Observational evidence for this has recently been reported, with Richards et al. (2004) identifying strong line profile variability in the gravitationally lensed quasar SDSS J1004+4112 which they attribute to the action of microlensing. If, as suggested by Bottorff & Ferland (2001), the broad line region of quasars also possesses fractal structure, it too may be susceptible to the influence of gravitational microlensing. Given its size, however, this region will cover the complex caustic network seen in microlensing, and the simple analysis presented in this paper will not apply. Requiring numerical simulation of high optical depth microlensing (Kayser, Refsdal & Stabell 1986; Wambsganss 1992), this will form the basis for further study.

ACKNOWLEDGEMENTS

GFL thanks Zdenka Kuncic for enlightening discussions on the generation of X-rays in quasars and for suggestions that improved the clarity of this paper. The anonymous referee is also thanked for comments which improved the paper.

REFERENCES

- Abajas C., Mediavilla E., Muñoz J. A., Popović L. Č., Oscoz A., 2002, *ApJ*, 576, 640
- Abramenko V. I., 1999, *ARep*, 43, 622
- Alcock C., Akerloff C. W., Allsman R. A., et al., 1993, *Nature*, 365, 621
- Alcock C., Allsman R. A., Alves D., et al., 2000, *ApJ*, 541, 270
- Agol E., Jones B., Blaes O., 2000, *ApJ*, 545, 657
- Burlaga L. F., Wang C., Ness N. F., 2003, *GeoRL*, 30, 50
- Bottorff M. C., Ferland G. J., 2000, *MNRAS*, 316, 103
- Bottorff M., Ferland G., 2001, *ApJ*, 549, 118
- Campo Bagatin A., Martínez V. J., Paredes S., 2002, *Icar*, 157, 549
- Chang K., 1984, *A&A*, 130, 157
- Dai X., Chartas G., Agol E., Bautz M. W., Garmire G. P., 2003, *ApJ*, 589, 100
- Datta S., 2003, *A&A*, 401, 193
- Durrer R., Labini F. S., 1998, *A&A*, 339, L85
- Elmegreen B. G., 1997, *ApJ*, 477, 196
- Elmegreen B. G., 2002, *ApJ*, 564, 773
- Elmegreen B. G., Elmegreen D. M., 2001, *AJ*, 121, 1507
- Elmegreen B. G., Kim S., Staveley-Smith L., 2001, *ApJ*, 548, 749
- Fluke C. J., Webster R. L., 1999, *MNRAS*, 302, 68

- Fogel M. E., Leung C. M., 1998, *ApJ*, 501, 175
 Goodwin S. P., Whitworth A. P., 2004, *A&A*, 413, 929
 Janßen K., Vögler A., Kneer F., 2003, *A&A*, 409, 1127
 Kayser R., Refsdal S., Stabell R., 1986, *A&A*, 166, 36
 Kochanek C. S., 2004, *ApJ*, 605, 58
 Lekshmi S., Revathy K., Prabhakaran Nayar S. R., 2003, *A&A*, 405, 1163
 Lewis G. F., Belle K. E., 1998, *MNRAS*, 297, 69
 Lewis G. F., Ibata R. A., 2004, *MNRAS*, 348, 24
 Lewis G. F., Irwin M. J., Hewett P. C., Foltz C. B., 1998, *MNRAS*, 295, 573
 Merloni A., Fabian A. C., 2001a, *MNRAS*, 321, 549
 Merloni A., Fabian A. C., 2001b, *MNRAS*, 328, 958
 Nemiroff R. J., 1988, *ApJ*, 335, 593
 Peitgen, H.-O., Saupe, D., 1988, *The Science of Fractal Images*, Springer-Verlag (Berlin)
 Peitgen, H.-O., Richter, P. H., 1986, *The Beauty of Fractals*, Springer-Verlag (Berlin)
 Popović L. Č., Mediavilla E. G., Jovanović P., Muñoz J. A., 2003, *A&A*, 398, 975
 Rauch K. P., Blandford R. D., 1991, *ApJ*, 381, L39
 Richards G. T. et al., 2004, *ApJ*, 610, 679
 Salakhutdinova I. I., 1998, *SoPh*, 181, 221
 Schneider P., Wagoner R. V., 1987, *ApJ*, 314, 154
 Schneider P., Wambsganss J., 1990, *A&A*, 237, 42
 Semelin B., Combes F., 2002, *A&A*, 387, 98
 Stenflo J. O., Holzreuter R., 2003, *AN*, 324, 397
 Stepinski T. F., Marinova M. M., McGovern P. J., Clifford S. M., 2002, *LPI*, 33, 1347
 Stutzki J., Bensch F., Heithausen A., Ossenkopf V., Zielinsky M., 1998, *A&A*, 336, 697
 Veronig A., Messerotti M., Hanslmeier A., 2000, *A&A*, 357, 337
 Wambsganss J., 1992, *ApJ*, 386, 19
 Wambsganss J., Paczynski B., Katz N., 1990, *ApJ*, 352, 407
 Witt H. J., 1990, *A&A*, 236, 311
 Wright E. L., 1989, *ApJ*, 346, L89
 Wyithe J. S. B., Loeb A., 2002, *ApJ*, 577, 615
 Wyithe J. S. B., Webster R. L., Turner E. L., 2000, *MNRAS*, 318, 762
 Yonehara A., 2001, *ApJ*, 548, L127
 Yonehara A., Mineshige S., Fukue J., Umemura M., Turner E. L., 1999, *A&A*, 343, 41
 Yonehara A., Mineshige S., Manmoto T., Fukue J., Umemura M., Turner E. L., 1998, *ApJ*, 501, L41